Numerical prediction and experimental verification of cavitation of Globe type Control Valves

S. Rammohan
Fluid Control Research
Institute, Palakkad, INDIA

S. Saseendran
Fluid Control Research
Institute, Palakkad, INDIA

S. Kumaraswamy
Mechanical Engineering Dept.,
IIT Madras, INDIA

ABSTRACT

Globe valves are one of the oldest types of valve used for throttling applications for all sizes due to better controllability and wider range. One of the major limitations associated with the use globe valves in liquid application is cavitation and it takes place both in part open and in fully open conditions due to varied reasons. There are different designs of globe valves available but for control valve applications, cage and plug designs are widely employed. Cage and plug design consists of body, valve cage, plug and an actuating mechanism. Actuating mechanism is connected to the valve plug which is a moving part, through valve shaft. There are many investigations reported about the flow visualization and numerical simulation of normal type globe valves. But study on valves with cage and plug design are not reported in detail. The objective of the present study is to provide a three dimensional analysis of flow through a globe valve with cage and plug design with emphasis on the inception and development of cavitation in detail. Cavitation reduction is achieved by breaking the flow in the form of more than one liquid jet, thereby increasing the turbulence inside the valve flow path. The numerical simulation was done using *GAMBIT* to set up geometry and grid and *FLUENT* to solve difference equation postulated from the conservation of mass and momentum of the fluid in motion. The k-epsilon model was used for turbulence. Results of five configurations of the cage with constant flow areas and valve stroke are presented in this paper. The numerical results were verified with an experimental program employing total flow measurement and pressure drop created by the valve at full opening. The study was conducted for different jet configurations to generalize the results of the study. Experimental validation was done in the water test facility with an operating pressure of 1.6 MPa and flow rate of 0.05 m^3/s. In the study, total area of opening for the flow and the valve stroke were kept constant. Accelerometers and dynamic pressure sensors were employed to sense the severity of cavitation at different differential pressures across the test valve.

INTRODUCTION

Valves are widely used in irrigation, energy, water distribution networks and process industries and in many other areas. Among the different types of valves used in the process industry, control valves play a vital role in the functioning and profitability of the plant. Trouble-free operation of control valves in the piping network is essential to avoid a situation leading to the total closure of the concerned industrial activity. Further, their efficient working leads to an effective use of the available resources. The abundant improvements in the design and performance of control valves are still insufficient to claim perfection in the agreement of theory and practice. The phenomenon of cavitation in control valves is the one in which some more progress can be achieved.

Globe valves are widely used for throttling applications in the process industry for both liquid and gaseous applications. The main advantages are relatively low cost, linear characteristics and good controllability and wider range. To obtain the required flow and pressure drop characteristics for the valves, different types of internals have been evolved for globe type valves. Cage and plug internal is one among them. One of the major limitations associated with the use of globe valves in liquid application is cavitation. This limits the operating regime of valves. To combat cavitation in valves, valve manufactures have evolved different solutions including design improvement, use of harder materials to reduce erosion rate, limiting the valve operation to some critical values so that downstream pressure never goes below vapour pressure etc.

Numerical models of Brennen [1], Wang & Brennen [2] and Davis & Stewart [3, 4] can be combined with two-phase flow starting after the convergent section of the nozzle. The starting of the flow is to be initiated by static pressure going below a threshold value. This value can be correlated to the local static pressure experienced in the valve. Ramamurthi & Nandakumar [5] studied characteristics of flow in the separated, attached and cavitated flow of small sharp edged cylindrical orifices. They have reported that the onset of cavitation observed is dependent on the diameter and aspect ratio of the orifices under study. They have studied on orifice plates with diameters varying from 0.3 to 2 mm. This study was extended by Ramamurthy and Patnaik [6] to investigate the effect of periodic disturbance present in the flow on the inception of cavitation. Cavitation characteristics of orifices were studied by Takehashi et al [7]. The spatial distribution of cavitation pressure downstream of the orifice along the pipe line was studied here. Cavitation of butterfly valve downstream of a multi holed orifice was also investigated in this study. Ishimoto & Kamiyama [8] described the numerical analysis of cavitating flow of a magnetic fluid in a vertical nozzle. Galson et al [9] modeled flow through venturi tube using bubble dynamics for

two phase analysis. Merati et al [10] described a method of numerical analysis as applied to flow through a v-sector ball valve. The experimental techniques employed for cavitation studies and the mode of result interpretation are described in detail by Tullis [11, 12].

NUMERICAL SIMULATION

Multi phase cavitation enabled mixture, RNG k-epsilon model was employed for analysis. The flow was governed by continuity and momentum equations with turbulence and multiphase (cavitation) modeling. Flow, volume fraction and turbulence equations were solved for the study. Following assumptions are made in the cavitation model:

- The system under investigation involves only two phases (a liquid and its vapor), and a certain fraction of separately modeled non-condensable gases.
- Both bubble formation (evaporation) and collapse (condensation) are taken into account in the model.
- The mass fraction of non-condensable gases is known in advance.

The summary details of the boundary conditions and the solver details of simulation employed for the solution of the present problem is shown in Table 1. The working fluid is assumed to be a mixture of liquid, vapor and non-condensable gases. Standard governing equations in the mixture model and the mixture turbulence model describe the flow and account for the effects of turbulence.

A vapor transport equation governs the vapor mass fraction, f, given by:

$$\frac{\partial}{\partial t}(\rho f) + \nabla(\rho \vec{v_v} f) = \nabla(\gamma \nabla f) + R_e - R_c \quad - \quad (1)$$

where ρ is the mixture density, $\vec{v_v}$ is the velocity vector of the vapor phase, γ is the effective exchange coefficient, and R_e and R_c are the vapor generation and condensation rate terms (or phase change rates). The rate expressions are derived from the Rayleigh-Plesset equations, and limiting bubble size considerations (interface surface area per unit volume of vapor).

When the local pressure p is less than the saturation pressure corresponding to the water temperature, vapourisation of liquid takes place and the rate of evaporation, R_e given by,

$$p < p_{sat} \qquad R_e = C_e \frac{V_{ch}}{\sigma} \rho_l \rho_v \sqrt{\frac{2(p_{sat} - p)}{3\rho_l}}(1 - f) \quad - \quad (2)$$

Where C_e is a constant, V_{ch} is the critical velocity at that pressure & temperature, σ is the surface tension of liquid, ρ_v is the vapour density, ρ_l is the liquid density, psat is saturation pressure corresponding to operating temperature and f is the vapour mass fraction. When liquid enters the region of higher pressure implosion of bubble takes place and the rate of condensation, Rc, is given by,

$$p > p_{sat} \qquad R_c = C_c \frac{V_{ch}}{\sigma} \rho_l \rho_l \sqrt{\frac{2(p - p_{sat})}{3\rho_l}} f \quad - \quad (3)$$

Where C_c is a constant.

Table 1 Boundary conditions and solver details

Model settings

Space	3D		
Time	Steady		
Viscous	RNG k-epsilon turbulence model		
Wall Treatment	Standard Wall Functions		
Multi phase	Mixture model (cavitation enabled)		

Boundary Conditions

Zones:

Inlet/outlet	Pressure-inlet/outlet	
Wall	No slip condition	

Solver Control Equations

Flow	yes
Volume Fraction	yes
Turbulence	yes

Material Properties

Material: air (fluid)

Density	kg/m^3	constant	1.225
C_p (Specific Heat)	J/kg-K	constant	1006.43
Thermal Conductivity	W/m-K	constant	0.0242
Viscosity	kg/m-s	constant	1.7894e-05

Material: water-liquid (fluid)

Density	kg/m^3	constant	995.59998
C_p (Specific Heat)	J/kg-K	constant	4182
Thermal Conductivity	W/m-K	constant	0.6
Viscosity	kg/m-s	constant	0.000798

Material: water-vapor (fluid)

Density	kg/m^3	constant	0.5542
C_p (Specific Heat)	J/kg-K	constant	2014
Thermal Conductivity	W/m-K	constant	0.0261
Viscosity	kg/m-s	constant	1.34e-05

FLUENT Release: 6.1.18

3D, segregated, Mixture, RNG k-epsilon were employed

DETAILS OF VALVE TESTED

The type of valve used for the study was a normal 75 mm nominal bore (NB) Globe type control valve with cage and plug design. These types of valves are prone for cavitation in the liquid applications. Figure 1 shows a valve cage with 4 holes drilled with combination plug. The diameter of the holes drilled were 17.5 mm with an effective total flow area of 981.11 mm^2. For the numerical studies, the valve was connected to pipe at both ends as shown in Figure 2.

Figure 1 Details of valve body, cage and plug

2

The diameter of the pipe and the thickness of the valve were same for the model and the one used for experimentation. Upstream and downstream lengths considered for the experimental set up were 750 and 1500 mm corresponding to 10 and 20 diameters of the pipe. This was selected so that the flow is fully developed at the valve inlet and full pressure recovery takes place in the pipe after the valve. Five different configurations of the valve internals were employed during simulation. Table 2 shows the details of orifices provided in the cage of the valve for simulation and experimental purpose. In all the configurations, the flow area and height of the openings were kept constant. During analysis, valve was kept in full open condition.

Table 2 Details of orifices in cage			
Total area = 981.1 mm^2			
Height of hole (h) = 17.5 mm			
Sl. No.	No. of orifices	Diameter of orifice(d)	
1	4	17.50	
2	6	10.50	
3	8	7.60	
4	12	4.87	

Cavitation simulation studies were carried out using *FLUENT*, finite volume based CFD Package. Multiphase simulation is carried out in order to simulate the flow through the valve and to find out the region in which cavitation occurs & for quantifying the intensity by means of the void fraction parameter. The mesh consists of about 1001684 cells with a higher resolution in proximity of valve gaps zone. The flow is governed by continuity and momentum equations with turbulence and multiphase (cavitation) modeling. Detail of the meshing is shown in Fig.2. $P_{in}(P_1)$ is the stagnation pressure at the inlet of the pipe. $P_{out}(P_2)$ is the static pressure at 20 pipe diameters downstream of test valve. During numerical analysis, the static pressure P_1 and P_2 were kept constant with varying flow rate. V_{in} is the incoming velocity in Z direction.
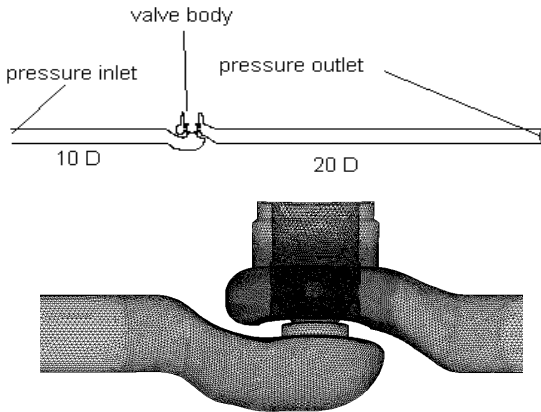
Figure 2 Valve configuration and meshing details

Water entering the pipe and leaving the pipe were assumed to contain no vapour. The amount of non-condensable gases present was assumed to be $1.5*10^{-05}$. During simulation, P_1 was varied from 100 kPa(g) to 1.4 MPa(g). The downstream pressure P_2 was maintained constant at 5.0 kPa(g). During simulation, single phase model was employed till the minimum

static pressure in flow field reaches close to vapour pressure. Then, two phase mixture model with cavitation enabled was used. By monitoring the vapour fraction (percentage vapour present in mixture) and static pressure, cavitation zone was identified and are explained in results. This was done for all the cage and orifice configurations described in Table 2. The method of conducting the simulation initially with single phase model and then extending it to two phase model with cavitation lead to a reduction in the computation time.

EXPERIMENTAL SET UP

A series of experiments were performed on a 75 mm NB globe valve with cage plug details described in Table 2 to validate the simulation results. The schematic of the experimental test setup is shown in Fig.3. The test setup was designed as per Tullis [11, 12]. It is an open loop re-circulating system which includes an underground sump that holds about 300 cubic meters of water, a 150 kW, multi stage centrifugal pump and valves to control and bypass the flow.

Water at ambient temperature was pumped with a maximum flow rate of 0.05 m^3/s at a head of 140 m. Flow rate and static pressure in the test loop were controlled with a by pass valve arrangement provided at the discharge of the pump. Flow rate through the loop was measured with a flow meter (100 mm orifice flow meter) provided upstream of the test valve. The outlet of the test valve was connected to the sump with a control valve in the loop. With this outlet pressure of the test valve can be controlled. The required differential pressure was created across the test valve by adjusting the bypass and control valves provided in the loop. The test valve opening was controlled by manually opening/closing the valve and measuring the valve stroke with a calibrated dial gauge.

Pressure gauge was used to measure the static pressure at the inlet of the test valve. The pressure/vacuum at the outlet of the test valve was monitored using a compound gauge. A Quartz type differential pressure transducer was used to measure the differential pressure across the test valve. Pressure tapings are provided one pipe diameter (1D) upstream and six pipe diameters (6D) down stream of the test valve. Pressure
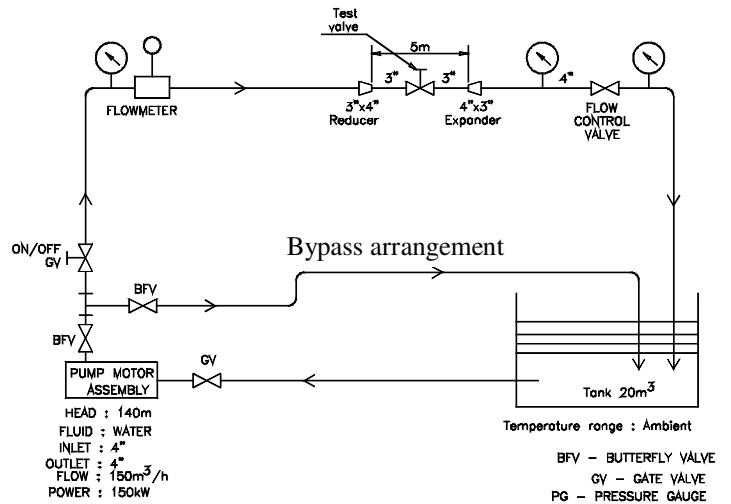

Figure 3 Schematic of experimental set up

tapings were also provided at a pitch of one pipe diameter, downstream of the test valve upto 750 mm. The pressure drop created by the valve for a specific flow rate at a particular valve opening, was determined by measuring the differential pressure across the valve between 1D & 6D pressure tapings. Calibrated pressure transducer was used for the discharge pressure measurement. Water temperature inside the pipe was measured using resistance temperature detector. The pressure upstream of the test valve was controlled with the bypass valve provided in the loop. Care was taken to avoid cavitation taking place in the bypass and downstream control valves of the loop. The dissolved oxygen in the loop was also monitored.

A quartz type dynamic pressure transducer was placed downstream of the test section to measure the pressure fluctuations in the flow. This was positioned flush with the pipe. Accelerometers were mounted on the test valve and pipe downstream of the test valve to sense vibration caused by cavitation. Mounting was done with suitable studs supplied along with the accelerometer. Fast Fourier Transform (FFT) analysis was performed on the collected signals to determine the dominant frequencies. After the water leaves the test section, it is routed back to the sump. Care was taken to ensure full running of the pipe during experimentation.

Uncertainties in the measurement of various parameters are listed in Table 3.

Table 3 Measurement uncertainties			
Sl. No.	Parameter	Range/ Sensitivity	Measurement uncertainty
1	Static pressure	0 – 2.0 MPa	± 1 %
2	Static pressure	100 – 200 kPa	± 1 %
3	Dynamic pressure	19.93 pC/bar	± 1 %
4	Vibration	0.050 pC/g	± 2 %
5	Flow	0 – 0.06 m³/s	± 0.5 %
6	Temperature	0 – 50 C	± 0.2 %
7	Dissolved oxygen	0-20 mg/l	± 2 %
8	Data acquisition	200 kHz	± 0.5 %

RESULTS

During simulation, flow rate through the valve, turbulent kinetic energy, vapour fraction (ratio of vapour phase in the mixture), mixture density and velocity of vapour were analysed. These were performed for varying differential pressure across the valve and different valve internal configurations. Of this, vapour fraction, mixture density and velocity of the vapour phase are employed in the vapour transport equation for simulation.
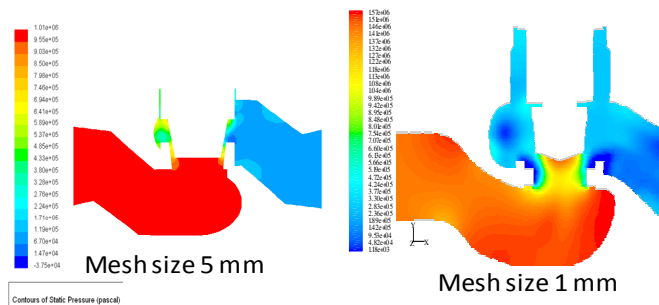
Figure 4 Effect of mesh size on the simulation results. Basic design, 1.0 MPa differential pressure

To study the effect of mesh size on the accuracy of prediction, simulation was performed with 10, 5, 1 mm mesh size throughout the simulated length. Figure 4 shows the results the analysis with static pressure as simulation parameter for two sizes of the mesh. It was observed that mesh size less than 1 mm is required for areas where cage and plug are close to one another. Hence during simulation varying mesh sizes were employed. Mesh close to plug and cage wall was maintained at 0.1 mm and it was increased to 5 mm at the pipe away from valve.

During experimentation, flow rate, vibration and hydraulic pressure fluctuations created due to cavitation were monitored by varying differential pressure across the valve and different valve internal configurations.

Figure 5 shows the plot of Valve capacity factor defined as

$$C_v = Q/DP^{0.5}$$

Valve capacity factor obtained from simulation and from experiment were plotted in Fig.5 as a function of number of holes. It may be noted that the difference between these are within 2%.
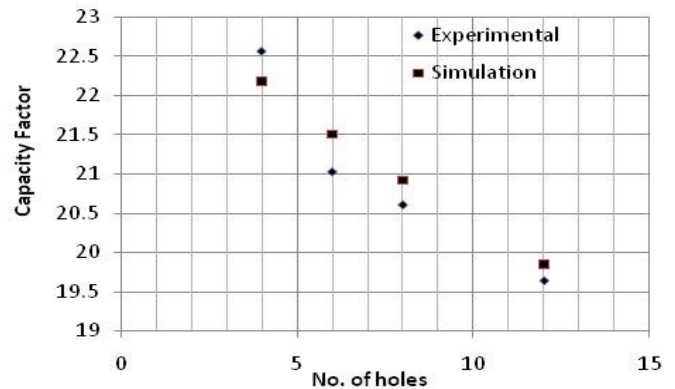

Figure 5 Plot of capacity Factor as a function of No. of holes

Table 4 shows the results of single phase simulation

Table 4 Single phase simulation results					
Diff. Pres.	Configuration	4 hole	6 hole	8 hole	12 hole
100 kPa	Flow (kg/s)	6.44	6.20	5.82	5.74
	Min. static Press. (Pa)	50578	56185	58911	65881
200 kPa	Flow (kg/s)	9.28	8.60	8.20	8.14
	Min. static Press.(Pa)	9255	15216	30890	33215
300 kPa	Flow (kg/s)	11.38	10.60	10.08	9.87
	Min. static Press.(Pa)	--	--	5100	7956

performed on the valve. Here as the differential pressure across the test valve increases, the static pressure goes below the vapour pressure and valve starts cavitating locally. It may be observed that differential pressure at which the cavitation behavior starts increases with number of holes. This, in conjunction with reduction in flow rate shows that there can be an optimum configuration with number of holes, valve capacity

4

and cavitation inception. Figure 6 shows the plot of absolute pressure and velocity contours obtained using single phase simulation.
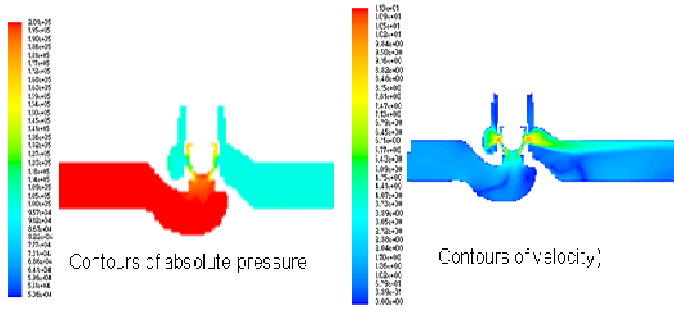

Figure 6 Contours of flow parameters DP=1 bar, Basic valve, Single phase model

Simulation was continued with multi phase mixture model with cavitation enabled. Here the vapour fraction, density of mixture and turbulent kinetic energy were observed as cavitation parameter. The simulation was performed for different percentage of non-condensable gases present in the liquid at inlet. For comparison with experimental results, mass fraction of non-condensable gas was taken as $1.5*10^{-5}$.

Figure 7 shows the variation of vapour fraction inside the valve as a function of differential pressure for the basic cage configuration. It can be seen that with increase in pressure differential, area of formation of vapour increases. However, this can be used for qualitative analysis of cavitation only. Hence turbulent kinetic energy and product of mixture density and vapour fraction (as seen in Equation 1) were employed for quantitative study.
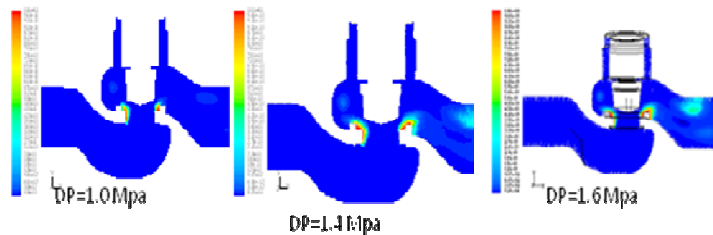
Figure 7 Contours of vapour fraction as a function of pressure across valve

Figure 8 shows the plot of the overall root mean square value of vibration and hydraulic pressure variations caused by cavitation measured using an accelerometer and dynamic pressure sensor. The measurements were done for varying differential pressure across the test valve. This was done for all the last four configurations mentioned in Table 2. Simulation parameters, turbulent kinetic energy (k) and the product of vapour fraction and mixture density ($\Sigma fv*\rho_m$) are also plotted in the same graph. The variation in parameters were plotted as a function of non-dimensional cavitation parameter σ defined as σ = $(P_1 – P_v)/(P_1 - P_2)$. The plot in Fig.8 was made for a cage with 12 orifices and valve in full open condition. It may be observed that both experimental parameters and simulation parameters as described above behave in a similar manner.

It can be seen that both experimental and theoretical values shows a similar trend as the σ is varied. In the theoretical analysis, the change is smooth whereas it is not so in the case of experimental results. The change in slope of vibration/dynamic pressure fluctuation defines change in cavitation behavior of the valve. The same behavior was obtained for other simulation parameters as well.
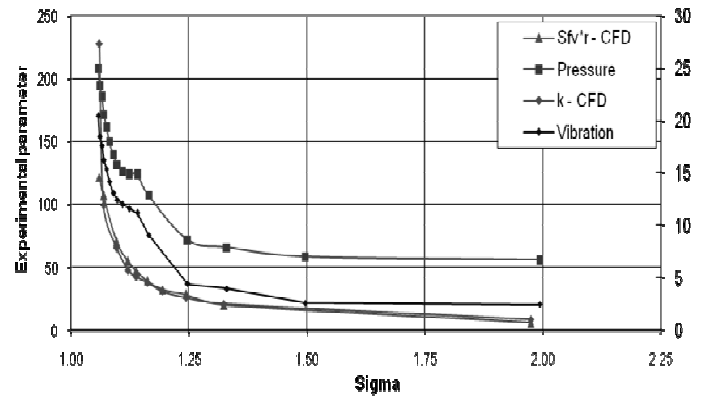

Figure 8 Plot of experimental results of acceleration and pressure fluctuation along with CFD results (No.of holes 12, opening: 100%)

It may be noted that a smooth transition of slope was obtained for simulation parameters whereas smooth behavior is not obtained from experimental results. The presence of cavitation was ensured by performing Fast Fourier Transform analysis of vibration and pressure fluctuations to obtain the frequency spectra.

DISCUSSION

Cavitation in control valves are characterized by the change in slope of vibration or pressure fluctuations graph plotted on a semi-log plot against non-dimensional differential pressure σ. In Figure 8, two simulation parameters, k and ($\Sigma fv*\rho_m$) were plotted along with vibration and pressure fluctuation measurements done on 75 mm NB valve for a typical orifice configuration. The variation of simulation parameters was very close to experimental parameters. Similar trends were obtained for other cage configurations discussed in Table 2.

CONCLUSION

A 75 mm NB valve was analysed for flow capacity and cavitation performance using numerical simulation with CFD package *FLUENT*. Five different cage configurations were tried to study the effect of prediction accuracy on valve configuration. Sufficient upstream and downstream lengths of pipe were provided for fully developed flow. Simulation was performed for varying differential pressure across the valve. The flow rate, turbulent kinetic energy, vapour fraction of vapour phase and mixture density were monitored during simulation.

To validate the simulation results, experiments were conducted on a 75 mm NB globe valve with same cage and plug configurations employed in simulation. The overall root mean square values of vibration of valve and hydraulic pressure fluctuations created by cavitation were used to study the cavitation characteristics of the valve. The valve capacity factor was employed to study the flow behavior.

Non-dimensional differential pressure (σ Vs k & σ Vs $\Sigma f_v * \rho_m$) plot of simulation results and experimental results were made. Both experimental and simulation results showed similar trend as shown in Fig. 8. Difference in the flow capacity obtained experimentally and using simulation matches within 2% as shown in Fig.5.

This study has revealed that irrespective of the cage configuration, there is a match in the trend of cavitation observed using simulation and experiment. Hence this method can be employed for cavitation analysis without subjecting the valve for cavitation test.

ACKNOWLEDGMENTS

NOMENCLATURE

C_c	Empirical constant (Condensation)	-
C_e	Empirical constant (Vapourisation)	-
C_v	Valve capacity factor $(Q/DP^{0.5})$	-
D	Pipe diameter	(mm)
d	Width of hole	(mm)
DP	Differential pressure across test valve	(kg/cm^2)
FFT	Fast Fourier Transform	
f, f_v	Vapour fraction	%
h	Height of orifice	(mm)
k	Turbulent kinetic energy	(m^2/s^2)
NB	Nominal Bore	(mm)
P	Pressure	(kPa)
P_{in}, P_1	Pressure at inlet of valve	(kPa)
P_{out}, P_2	Pressure at outlet of valve	(kPa)
P_{sat}	Saturation pressure	(kPa)
P_v	Liquid vapour pressure	(kPa)
Q	Flow rate	(m^3/h)
R_c	Vapour condensation rate term	-
R_e	Vapour generation rate term	-
V_{ch}	Critical velocity	(m/s)
V_{in}	Incoming velocity in Z direction	(m/s)
v_v	Velocity of the vapour phase	(m/s)
γ	Effective exchange coefficient	-
ρ	Fluid density	(kg/m^3)
ρ_l	Density of the liquid	(kg/m^3)
ρ_m	Density of the mixture	(kg/m^3)
ρ_v	Density of the vapour	(kg/m^3)
σ	Cavitation index $(P_1-P_v)/(P_1-P_2)$	-

REFERENCES

[1] Brennen, C.E. 1995, *Cavitaion & bubble dynamics*, Oxford University Press.

[2] Wang, Y.C. and Brennen, C.E. 1998, "One–dimensional cavitation flow through a converging diverging nozzle", *Trans. ASME J. of Fluids Engineering.*, 120, 166-170.

[3] Davis, J.A. and Stewart, M. 2002, "Predicting globe control valve performance—Part I: CFD modeling," *Trans. ASME J. of Fluids Engineering*, 124, 772-777.

[4] Davis, J.A. and Stewart, M. 2002, "Predicting globe control valve performance—Part II: Experimantal verification," *Trans. ASME J. of Fluids Engineering*, 124, 778-783.

[5] Ramamurthi, K. and Nandakumar, K. 1999, "Characteristics of flow through small sharp edged cylindrical orifices", *Flow Measurement & Instrumentation*, 10, 133-143.

[6] Ramamurthi, K. and Patnaik, S.R. 2003, "Influence of periodic disturbance on inception of cavitation in sharp edged orifices", *Experiments in Fluids*, 33, 720-727.

[7] Takehashi, K., Matsuna, H. and Miyamoto, H. 2001, "Cavitation characteristics of restriction orifices", Proc. of 4th international symposium on cavitation, CAV 2001.

[8] Ishimoto, J. and Kamiyama, S. 2005, "Numerical study of cavitating flow of magnetic fluid in a vertical converging-diverging nozzle", *J. of Magnetism and Magnetic Materials*, 289, 260-263.

[9] Gaslon, M.J., Reize, J.A. and Evan, G.M. 2001, "Modeling of bubble dynamics in a venturi flow", *Chemical Engg. Science*, 56, 6427-6435.

[10] Merati, P., Macelt, M.J. and Erickson, R.B. 2001, "Flow investigation around a v-sector ball valve" *Trans. ASME J. of Fluids Engineering*., 123, 662-671.

[11] Tullis, J.P. 1974, "Testing valves for cavitation", Conf. on Cavitation organized by the Institution of Mechanical Engineers, London, 45.

[12] Tullis, J.P. 1993, "Cavitaion guide for control valves", Report No. NUREG/CR-6031-1993, US Nuclear Regulatory commission.